JOURNAL OF BACTERIOLOGY, Dec. 2011, p. 6425–6435 Vol. 193, No. 23
0021-9193/11/$12.00 doi:10.1128/JB.06003-11

Functional Characterization of the RuvB Homologs from *Mycoplasma pneumoniae* and *Mycoplasma genitalium*▽

Silvia Estevão, Marcel Sluijter, Nico G. Hartwig, Annemarie M. C. van Rossum, and Cornelis Vink*

Erasmus MC-Sophia Children's Hospital, Laboratory of Pediatrics, Pediatric Infectious Diseases and Immunity, 3000 CA Rotterdam, The Netherlands

Received 12 August 2011/Accepted 16 September 2011

Homologous recombination between repeated DNA elements in the genomes of *Mycoplasma* species has been hypothesized to be a crucial causal factor in sequence variation of antigenic proteins at the bacterial surface. To investigate this notion, studies were initiated to identify and characterize the proteins that form part of the homologous DNA recombination machinery in *Mycoplasma pneumoniae* as well as *Mycoplasma genitalium*. Among the most likely participants of this machinery are homologs of the Holliday junction migration motor protein RuvB. In both *M. pneumoniae* and *M. genitalium*, genes have been identified that have the capacity to encode RuvB homologs (MPN536 and MG359, respectively). Here, the characteristics of the MPN536- and MG359-encoded proteins (the RuvB proteins from *M. pneumoniae* strain FH [$RuvB_{FH}$] and *M. genitalium* [$RuvB_{Mge}$], respectively) are described. Both $RuvB_{FH}$ and $RuvB_{Mge}$ were found to have ATPase activity and to bind DNA. In addition, both proteins displayed divalent cation- and ATP-dependent DNA helicase activity on partially double-stranded DNA substrates. The helicase activity of $RuvB_{Mge}$, however, was significantly lower than that of $RuvB_{FH}$. Interestingly, we found $RuvB_{FH}$ to be expressed exclusively by subtype 2 strains of *M. pneumoniae*. In strains belonging to the other major subtype (subtype 1), a version of the protein is expressed (the RuvB protein from *M. pneumoniae* strain M129 [$RuvB_{M129}$]) that differs from $RuvB_{FH}$ in a single amino acid residue (at position 140). In contrast to $RuvB_{FH}$, $RuvB_{M129}$ displayed only marginal levels of DNA-unwinding activity. These results demonstrate that *M. pneumoniae* strains (as well as closely related *Mycoplasma* spp.) can differ significantly in the function of components of their DNA recombination and repair machinery.

A significant portion of the genomes of *Mycoplasma pneumoniae* and *Mycoplasma genitalium* consists of repeated DNA elements. This is remarkable as the genomes of these closely related human pathogens are relatively small, with lengths of 816 kb and 580 kb, respectively (6, 8). In *M. pneumoniae*, the repeated DNA elements are termed RepMP elements (29, 37, 44), whereas in *M. genitalium*, they are referred to as MgPa repeats (MgPars) (6, 26, 27). Although the RepMP elements and MgPa repeats do not have significant sequence homology, they do share two important features: (i) the different variants of these elements are similar in sequence but not identical, and (ii) one or more of these variants form part of open reading frames (ORFs) that code for antigenic surface proteins, such as the P1 protein in *M. pneumoniae* and the MgPa protein in *M. genitalium*. Because both P1 and MgPa can display sequence variation in the regions encoded by the RepMP or MgPar elements, it has been hypothesized that this variation is caused by homologous DNA recombination between the different variants of the RepMP or MgPar elements (10–11, 15, 17, 35, 36). Obviously, these recombination processes may supply a plethora of sequence variation to the P1 and MgPa genes, which can subsequently lead to amino acid sequence variation of the encoded antigenic proteins. Homologous DNA recombination between the repeated DNA elements in both *Mycoplasma* species may thus contribute significantly to evasion of these pathogens from the host's immune system.

It is probable that the enzymatic machinery that governs recombination between repeated DNA elements in *M. pneumoniae* and *M. genitalium* largely overlaps with the machinery that is involved in homologous DNA recombination and DNA repair in these bacteria. Sequence analysis of the genomes of both *M. pneumoniae* and *M. genitalium* has revealed the presence of a distinct and limited set of ORFs that may encode the core proteins involved in DNA recombination pathways (2, 6, 8). The activities of some of these putative core proteins have already been investigated. These proteins include RuvA and a single-stranded DNA (ssDNA)-binding protein (SSB) from *M. pneumoniae* (9, 32) and the RecA and RecU proteins from both *M. pneumoniae* and *M. genitalium* (31, 33, 34). While the first three proteins exhibited activities that are similar to those of their counterparts from other bacteria, the RecU proteins from both *Mycoplasma* species displayed unusual and unique characteristics. First, while RecU from *M. genitalium* ($RecU_{Mge}$) was found to bind and cleave Holliday junction (HJ) substrates in a specific fashion, the RecU protein from *M. pneumoniae* ($RecU_{Mpn}$) did not possess obvious DNA-binding or -cleavage activities. The inactivity of $RecU_{Mpn}$ was found to be caused by the presence of a glutamic acid residue at position 67 of the protein (33), which is not conserved in $RecU_{Mge}$ or any other known RecU-like sequence. In addition, $RecU_{Mpn}$ can be expressed only by a subgroup of *M. pneumoniae* strains (the so-called subtype 2 strains) and not by other strains (subtype 1 strains) as the latter strains contain a premature TAA

* Corresponding author. Mailing address: Erasmus MC, Laboratory of Pediatrics, P.O. Box 2040, 3000 CA Rotterdam, The Netherlands. Phone: 31 107044224. Fax: 31 107044761. E-mail: c.vink@erasmusmc.nl.

▽ Published ahead of print on 23 September 2011.

translation termination codon within the RecU gene (33). The apparent lack of a functional RecU protein in *M. pneumoniae* was hypothesized to be a possible cause of the relatively low level of homologous DNA recombination events in this bacterial species (33).

To further delineate the composition and characteristics of the DNA recombination machinery of *M. pneumoniae* and *M. genitalium*, the current study focused on the proteins encoded by ORFs MPN536 and MG359 from *M. pneumoniae* and *M. genitalium*, respectively. These ORFs were previously reported to show sequence similarity to the RuvB HJ branch migration motor proteins from other bacterial species (6, 8). Here, we show that the MPN536-derived protein from *M. pneumoniae* strain FH ($RuvB_{FH}$) is a potent DNA helicase, whose activity is dependent on ATP and divalent cations (Mg^{2+} or Mn^{2+}). Interestingly, the characteristics of $RuvB_{FH}$ differ significantly from those of the MPN536-encoded protein from *M. pneumoniae* strain M129 ($RuvB_{M129}$) and from the MG359-encoded protein from *M. genitalium* ($RuvB_{Mge}$).

MATERIALS AND METHODS

Strains. All *M. pneumoniae* strains used in this study, including reference strains FH (ATCC 15531), M129 (ATCC 29342), and PI 1428 (ATCC 29085), as well as *M. genitalium* strain G37 (ATCC 33530), were cultured in *Mycoplasma* medium, as described previously (18).

Cloning of the *M. pneumoniae* MPN536 gene and *M. genitalium* MG359 gene. Bacterial DNA was purified from cultures of *M. pneumoniae* and *M. genitalium* following standard procedures (32). The MPN536 ORF of *M. pneumoniae* strain FH was amplified by PCR. Although this ORF has recently been designated MPNE_0635 in the complete genome sequence of strain FH (GenBank accession number CP002077.1), we have maintained the name MPN536, which is derived from the published annotation of the genome sequence of strain M129 (3, 8). The PCR was performed using the following primers: RuvB_FW (5′-GGTCGT*CATATG*AAGTTACAAATAAAACCG-3′, which overlaps with the translation initiation codon [underlined] of MPN536) and primer RuvB_RV (5′-GCAGCC-*GGATCC*TTAGCAGCTAGTTAAATAATTAC-3′, which overlaps with the antisense sequence of the translation termination codon [underlined] of the gene). The resulting 0.9-kbp (kb) PCR fragment was digested with NdeI and BamHI (the recognition sites for these enzymes are indicated in italics in the sequences of primers RuvB_FW and RuvB_RV, respectively) and cloned into NdeI- and BamHI-digested vector pET-11c, resulting in plasmid pET-11c-$RuvB_{FH}$. In this plasmid, the MPN536 ORF is cloned such as to express the *M. pneumoniae* FH MPN536-encoded protein ($RuvB_{FH}$) in its native form in *Escherichia coli*.

The cloning of the *M. genitalium* MG359 ORF was performed using the following primers: RuvBmgpET_fw (5′-GCTGA*CATATG*AAATTACAAATAAAACCGCCT-3′ which includes an NdeI restriction site [in italics] and the translation initiation codon of MG359 [underlined]) and RuvBmgpEt_rv (5′-CAAGC*GGATCC*GCTAATAAGCTTAAAAGTTAAC-3′, which includes a BamHI site [in italics] and the antisense sequence of the translation termination codon [underlined] of the gene). The 0.9-kb PCR product was digested with NdeI and BamHI and ligated into NdeI- and BamHI-digested vector pET-11c, resulting in expression vector pET-11c-$RuvB_{Mge}$. From this construct, the *M. genitalium* MG359-encoded protein ($RuvB_{Mge}$) was expressed in its native form.

Generation of MBP fusion constructs. The plasmid expressing a maltose-binding protein (MBP)-$RuvB_{FH}$ fusion was generated as follows. First, a PCR was done using primers ruvb_pmal_fw (5′-GGT*GAATTC*ATGAAGTTACAAATAAAACCG-3′, which contains an EcoRI site [in italics] immediately 5′ of the start codon [underlined] of MPN536) and ruvb_pmal_rv 5′-GCA*CTGCAG*TTAGCAGCTAGTTAAATAATTAC-3′, which contains a PstI site [in italics] and the antisense sequence of the translation termination codon [underlined] of MPN536, using plasmid pET-11c-$RuvB_{FH}$ as a template. The resulting fragment was digested with EcoRI and PstI and ligated into the EcoRI- and PstI-digested vector pMAL-c (New England BioLabs), yielding plasmid pMALc-$RuvB_{FH}$. This plasmid was employed for the expression of $RuvB_{FH}$ as a carboxyl-terminal fusion to MBP (MBP-$RuvB_{FH}$). By using a similar protocol, expression plasmid pMALc-$RuvB_{M129}$ was constructed. In this plasmid, the TGA codon that encodes Trp140 of $RuvB_{M129}$ was modified into a TGG codon by a PCR-based procedure; this change was required for expression of the full-length protein in *E. coli*.

Plasmid pMALc-$RuvB_{Mge}$ was generated by a method similar to that used for pMALc-$RuvB_{FH}$ and pMALc-$RuvB_{M129}$. In the initial PCR, plasmid pET-11c-$RuvB_{Mge}$ was used as template DNA in combination with primers RuvBmgp MAL_fw (5′-GCTGAGAATTCATGAAATTACAAATAAAACCGCCT-3′) and RuvBmgpMAL_rv (5′-CAAGCCTGCAGGCTAATAAGCTTAAAAGTTAAC-3′).

DNA sequencing. The integrity of all DNA constructs used in this study was checked by dideoxy sequencing, as described before (36). The complete sequences of the MPN536 ORFs from three *M. pneumoniae* subtype 1 strains (Mp72, Mp4817, and PI 1428) and three subtype 2 strains (Mp5181, Ofo, and R003), were determined using previously described procedures (33).

Expression and purification of $RuvB_{FH}$, $RuvB_{Mge}$, and MBP fusion proteins. Constructs pET-11c-$RuvB_{FH}$ and pET-11c-$RuvB_{Mge}$ were introduced into *E. coli* BL21(DE3), and the resulting strains were grown overnight at 37°C in LB medium containing 100 μg/ml ampicillin. Protein expression was induced as described before (34).

$RuvB_{FH}$ was purified as follows. The frozen bacterial pellet was resuspended in 20 ml of buffer A (20 mM Tris-HCl [pH 7.4], 0.1 M NaCl, 0.1 mM EDTA, 1 mM dithiothreitol [DTT]) containing 0.5 mg/ml of lysozyme. The suspension was sonicated on ice and clarified by centrifugation for 20 min at 12,000 × *g* (4°C). All subsequent purification steps were performed either on ice or at 4°C. The pellet, which contained ~60% of the expressed $RuvB_{FH}$ proteins, was resuspended in 20 ml of buffer B (20 mM Tris-HCl [pH 7.4], 1 M NaCl, 0.1 mM EDTA, 1 mM DTT). Then, the suspension was homogenized on ice using a Heidolph Potter homogenizer. After incubation on a roller bench for 1 h, the suspension was centrifuged for 20 min at 12,000 × *g*. The supernatant (20 ml) was dialyzed overnight to buffer A, after which the sample was diluted with buffer A to 45 ml. The sample was then added to 3 ml of Q Sepharose Fast Flow (GE Healthcare), which was previously equilibrated in buffer A. The suspension was incubated on a roller bench for 2.5 h, after which the unbound fraction, which contained the $RuvB_{FH}$ proteins, was subjected to affinity chromatography using Heparin Sepharose 6 Fast Flow (GE Healthcare) and single-stranded DNA-cellulose (Worthington Biochemical Corp., Lakewood, NJ). The $RuvB_{FH}$-containing fractions were pooled, dialyzed against a solution of 20 mM Tris-HCl (pH 7.4), 0.2 M NaCl, 0.1 mM EDTA, 1 mM DTT, and 50% glycerol and stored at −20°C. $RuvB_{Mge}$ was purified in a similar fashion as $RuvB_{FH}$.

The expression and purification of MBP fusion proteins have previously been described (31, 33). The purification of $RuvA_{Mpn}$ was reported by Ingleston and coworkers (9); this protein does not vary in sequence among *M. pneumoniae* subtype 1 and subtype 2 strains. The expression and purification of $RuvA_{Mge}$ will be reported elsewhere.

SDS-PAGE. Proteins were separated on SDS-polyacrylamide gels, essentially as described before (16). After electrophoresis, gels were stained with Coomassie brilliant blue (CBB), destained in 40% methanol–10% acetic acid, and photographed using a GelDoc XR system (Bio-Rad). Digital images were processed using Quantity One 1-D Analysis Software (Bio-Rad).

ATPase assays. The ATPase activities of the RuvB proteins were determined by using a β-NAD reduced form (NADH)-coupled assay on a VersaMax Tunable Microplate Reader (Molecular Devices), as described previously (19, 34).

DNA substrates. The DNA substrates that were used in the DNA helicase assays (see below) were previously described by Tsaneva and coworkers (40). The structures of these substrates are schematically depicted in Fig. 3A. They are composed of synthetic oligonucleotides alone (substrates V and VI) or of a combination of oligonucleotides and single-stranded, circular 5,386-bp φX174 DNA (substrates I to IV). The oligonucleotides were purchased from Eurogentec. The φX174 virion DNA was obtained from New England BioLabs.

DNA-binding assays. Binding of the RuvB proteins to supercoiled pBluescript SK^- DNA (Stratagene) and EcoRI-linearized pBluescript SK^- was carried out in 10-μl volumes and included 20 mM Tris-acetate (OAc), pH 7.5, 1 mM DTT, 20 ng of DNA, 1 mM ATPγS, and various concentrations of RuvB proteins. The binding to single-stranded oligonucleotide 1 (see Fig. 3A), double-stranded oligonucleotide substrate VI (see Fig. 3A), and Holliday junction (HJ) substrate HJ1.1 (33), which were each 5′-end labeled on a single strand with 6-carboxyfluorescein (6-FAM), was done similarly as described above, using a DNA concentration of 12.3 nM. After incubation for 30 min at 37°C, 1 μl was added of a solution containing 40% glycerol and 0.25% bromophenol blue. Then, the reaction mixtures were electrophoresed through either 0.6% agarose gels (when plasmid substrates were used) or 5% polyacrylamide gels (when oligonucleotide substrates were used) in 0.5× TBE buffer (45 mM Tris, 45 mM boric acid, 1 mM EDTA). Following electrophoresis, the agarose gels were stained with ethidium bromide and photographed using the GelDoc XR system. The polyacrylamide

gels were analyzed by fluorometry, using a Typhoon Trio 9200 Variable Mode Imager (GE Healthcare). Digital images were converted into TIFF files using the Typhoon Scanner Control, version 4.0, software (Amersham Bioscience) and processed using Quantity One 1-D Analysis Software.

DNA helicase assays. DNA helicase assays were performed with 5′ fluorescently (6-FAM)-labeled DNA substrates (see Fig. 3A for the structures of these substrates) and were analyzed by native polyacrylamide gel electrophoresis. Standard reaction mixtures (10 μl) contained 20 mM Tris-HCl, pH 7.5, 1 mM DTT, 50 ng/μl bovine serum albumin (BSA), 10 mM $MgCl_2$, 2 mM ATP, either 11.5 nM (for substrates I to IV) (see Fig. 3A) or 8 nM (for substrates V and VI) (see Fig. 3A) substrate DNA, and various concentrations of RuvB and RuvA proteins. Reactions were carried out for 5 min at 37°C, after which the reactions were terminated by the addition of 1 μl of Termination Mix (100 mM Tris-HCl, pH 7.4, 5% SDS, 0.2 M EDTA) and 1 μl of proteinase K (at 10 mg/ml). After deproteinization for 15 min at 37°C, 1.5 μl of loading dye (40% glycerol, 0.25% bromophenol blue) was added, and the samples were loaded onto a native 12% polyacrylamide–1× TBE mini-gel. Following electrophoresis, gels were analyzed by fluorometry, using the Typhoon Trio 9200 Variable Mode Imager. Digital images were processed as described above.

RESULTS

***M. pneumoniae* MPN536 and *M. genitalium* MG359 encode RuvB homologs.** The MPN536 ORF of *M. pneumoniae* and MG359 ORF of *M. genitalium* have previously been annotated as genes that potentially encode RuvB homologs (6, 8, 27). The similarity between the amino acid sequences encoded by MPN536 and MG359 and those of (putative) RuvB proteins from other bacterial species can readily be observed in a multiple sequence alignment (Fig. 1A). The similarity between the sequences from *M. pneumoniae* and *M. genitalium* is very high (84.4% identity). A significantly lower similarity is seen between the sequences from the *Mycoplasma* spp. and those from other bacterial species (Fig. 1A). Protein regions that are highly conserved among the RuvB proteins are found in the amino-terminal (N) and central (M) domains and include the Walker A and B motifs and the sensor I and II motifs (23, 45). These motifs are characteristic for proteins that belong to the so-called AAA^+ protein superfamily (ATPases associated with various cellular activities) (22). The Walker and sensor motifs are involved in the interaction with, and hydrolysis of, ATP (4). The RuvB region that was previously characterized as a β-hairpin 1 motif (Fig. 1A) is not highly conserved between the *Mycoplasma* RuvB sequences and the sequences of other RuvB proteins. In *E. coli* RuvB ($RuvB_{Eco}$), this motif was found to be important for the interaction of the protein with RuvA (7).

It is interesting that the MPN536-encoded amino acid sequences of *M. pneumoniae* reference strains M129 and FH differ by a single residue, at position 140 (Fig. 1A); at this position a tryptophan (Trp) residue is present within the M129 RuvB protein ($RuvB_{M129}$), and a leucine (Leu) is present within the FH protein ($RuvB_{FH}$). Although sequence differences can be observed throughout the genomes of these two strains, which are representative of the two major genotypes of *M. pneumoniae* (subtypes 1 and 2), the presence of a Trp residue at position 140 of $RuvB_{M129}$ is remarkable as all other known RuvB sequences contain a Leu at this position. Moreover, this Leu residue forms part of the highly conserved sensor II sequence (Fig. 1A). To investigate whether the sequences of $RuvB_{FH}$ and $RuvB_{M129}$ are representative for subtype 2 and subtype 1 strains, respectively, we determined the sequence of the MPN536 ORF from three additional subtype 2 strains (Mp5181, Ofo, and R003) and three subtype 1 strains (Mp72, Mp4817, and PI 1428) (36). While the sequences from the subtype 2 strains were all found to be identical to the MPN536 sequence from strain FH, the sequences from the subtype 1 strains were all identical to the M129 sequence. Due to the deviant nature of the RuvB sequence from subtype 1 strains, we initially decided to focus our attention on characterization of the RuvB variant that is expressed by subtype 2 strains ($RuvB_{FH}$).

Expression and purification of $RuvB_{FH}$ and $RuvB_{Mge}$. The MPN536 and MG359 ORFs were amplified by PCR and cloned into protein expression vector pET-11c. This vector was used for the expression of $RuvB_{FH}$ and $RuvB_{Mge}$ in their native forms in *Escherichia coli*. Both proteins were purified to near homogeneity using similar procedures (Fig. 1B). The estimated molecular masses of the purified proteins corresponded to their theoretical molecular masses of 35.0 kDa for both $RuvB_{FH}$ (Fig. 1B, lane 2) and $RuvB_{Mge}$ (lane 4).

$RuvB_{FH}$ and $RuvB_{Mge}$ possess ATPase activity. As described above, the predicted amino acid sequences of $RuvB_{FH}$ and $RuvB_{Mge}$ show all the characteristics of ATPases belonging to the AAA^+ protein family. To test whether these proteins can be classified as ATPases, their ability to hydrolyze ATP was tested in the presence of Mg^{2+} and single-stranded DNA. Although both $RuvB_{FH}$ and $RuvB_{Mge}$ were, indeed, found to possess ATPase activity under these conditions, the $RuvB_{FH}$ protein appeared to have a higher activity than $RuvB_{Mge}$ (Fig. 1C). Although the ATPase activity of the RuvB proteins is likely to depend on the nature and concentration of DNA and other reaction constituents, as was demonstrated previously for other RuvB proteins such as *E. coli* RuvB ($RuvB_{Eco}$) (13, 21), the influence of these factors was not investigated further.

DNA-binding activity of $RuvB_{FH}$ and $RuvB_{Mge}$. The ability of $RuvB_{FH}$ and $RuvB_{Mge}$ to bind DNA was first investigated using supercoiled plasmid DNA in an agarose-based electrophoretic mobility shift assay. As shown in Fig. 2, both proteins formed large DNA-protein complexes in a protein concentration-dependent manner in the presence of ATPγS. These complexes, some of which did not enter the gel (Fig. 2A and B, lanes 6 and 7), were similarly formed in the presence of ATP or in the absence of any nucleotide cofactor (data not shown). Moreover, the addition of divalent cations to the binding reaction mixtures (10 mM Mg^{2+} or 5 mM Mn^{2+}) did not significantly influence the binding characteristics of $RuvB_{FH}$ and $RuvB_{Mge}$ (data not shown). While the use of the cross-linking agent glutaraldehyde was shown to be required for stabilization and, as a consequence, detection of the complexes between *E. coli* RuvB and DNA (21), the use of glutaraldehyde did not have a significant effect on the nature of the complexes that were generated between plasmid DNA and either $RuvB_{FH}$ or $RuvB_{Mge}$.

Both $RuvB_{FH}$ and $RuvB_{Mge}$ were also found to bind to linearized plasmid DNA (data not shown) and to single-stranded (ssDNA), double-stranded (dsDNA), and Holliday junction (HJ) substrates; with each of these substrates, large DNA-protein complexes were produced that did not enter the gels (Fig. 2C to E and data not shown). Binding of $RuvB_{FH}$ to the HJ substrate resulted in the most stable complexes; cross-linking with glutaraldehyde did not have a significant effect on these complexes (Fig. 2C). In contrast, cross-linking did have a stabilizing effect on complexes formed between $RuvB_{FH}$ and

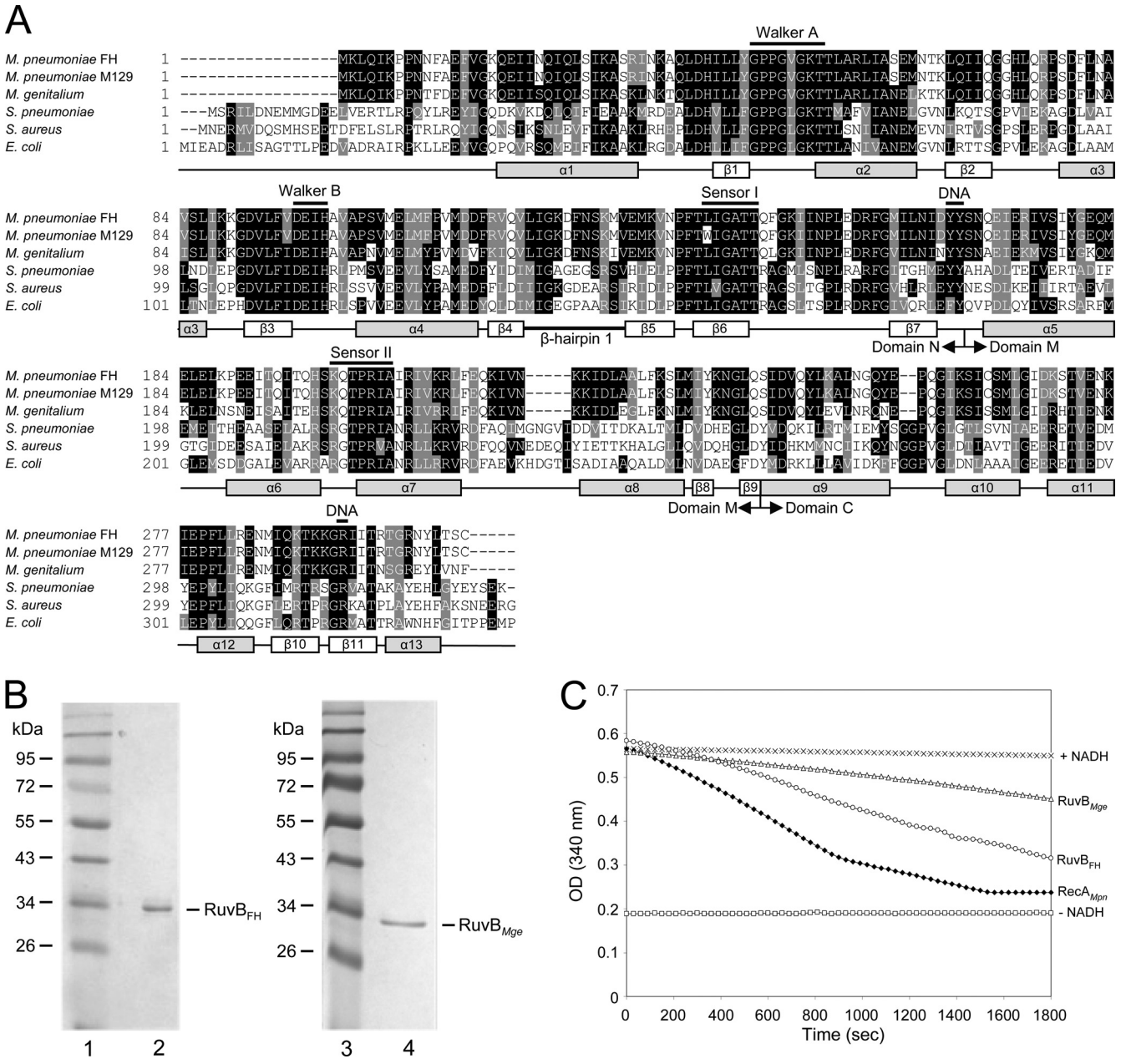

FIG. 1. Multiple alignment of RuvB sequences and ATPase activity of $RuvB_{FH}$ and $RuvB_{Mge}$. (A) A multiple alignment was generated with amino acid sequences predicted to be encoded by the following ORFs (with GenBank accession numbers in parentheses): *M. pneumoniae* FH MPN536 (ADK87167), *M. pneumoniae* M129 MPN536 (AAB95954), *M. genitalium* G37 MG359 (ZP_05405689), *Streptococcus pneumoniae ruvB* (Q97SR6), *Staphylococcus aureus ruvB* (NP_374754), and *E. coli ruvB* (P0A812). Predicted secondary structural features of the RuvB proteins are shown below the alignment and are based on the crystal structures of the RuvB proteins from *Thermus thermophilus* HB8 (45) and *Thermotoga maritima* (28). The annotation of the (predicted) α helices and β strands, as well as the boundaries of the amino-terminal (N), central (M), and carboxyl-terminal domains, is derived from Yamada et al. (45). The positions of crucial, conserved motifs of AAA^+ proteins, i.e., Walker A, Walker B, and sensor I and sensor II motifs, are indicated above the sequences. Amino acids potentially involved in DNA or nucleotide binding are also indicated (DNA) (12, 45).The multiple alignment was performed using Clustal W (http://www.ebi.ac.uk/Tools/msa/clustalw2/). The program BOXSHADE, version 3.21 (http://www.ch.embnet.org/software/BOX_form.html), was used to generate white letters on black boxes (for residues that are identical in at least three out of six sequences) and white letters on gray boxes (for similar residues). (B) Purification of $RuvB_{FH}$ and $RuvB_{Mge}$. Samples of purified $RuvB_{FH}$ (left panel, lane 2) and $RuvB_{Mge}$ (right panel, lane 4) were analyzed by SDS-PAGE (12%) and Coomassie brilliant blue (CBB) staining. The sizes of protein markers (lanes 1 and 3; PageRuler Prestained Protein Ladder [Fermentas]) are shown on the left-hand side of each panel in kDa. (C) ATPase activity of $RuvB_{FH}$ and $RuvB_{Mge}$. ATP hydrolysis by $RuvB_{FH}$ (○) and $RuvB_{Mge}$ (Δ) was measured at a protein concentration of 0.5 μM in the presence of Mg^{2+} (1 mM) and φX174 single-stranded DNA (1.5 nM). The ATPase activity was determined using an NADH-coupled assay. Using this assay, the activity is calculated from the stationary velocities of ATP hydrolysis as determined by monitoring the absorption of NADH at 340 nm (19, 34). The $RecA_{Mpn}$ protein, characterized previously by Sluijter et al. (34), was taken along as a positive control at a concentration of 0.5 μM (◆). Control reactions were performed in the absence of any protein (+NADH, ×) and in the absence of both NADH and protein (−NADH, □). OD, optical density.

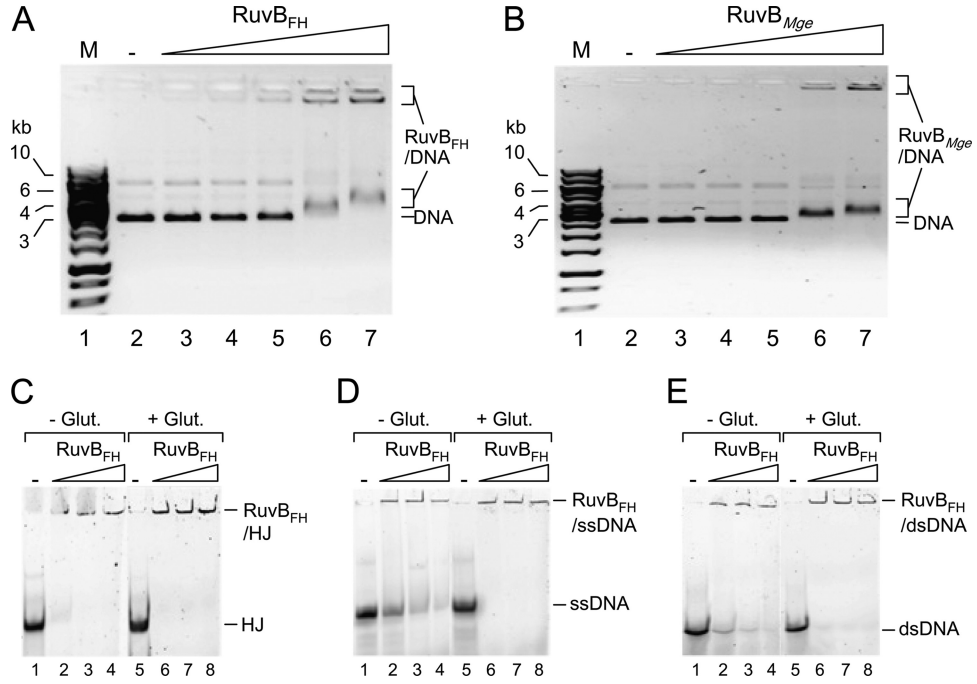

FIG. 2. DNA-binding activity of $RuvB_{FH}$ and $RuvB_{Mge}$. (A) Binding of $RuvB_{FH}$ to supercoiled plasmid DNA. The DNA-binding reactions were performed as indicated in Materials and Methods. In short, reactions were performed in volumes of 10 μl and contained 20 ng of DNA, 1 mM ATPγS, and either 0 nM (−; lane 2), 340 nM (lane 3), 680 nM (lane 4), 1.35 μM (lane 5), 2.7 μM (lane 6), or 5.4 μM (lane 7) $RuvB_{FH}$. The protein-DNA mixtures were separated by native 0.6% agarose gel electrophoresis, followed by staining with ethidium bromide. A black/white inverted image of the stained gel is shown. The positions of the unbound DNA (DNA) and $RuvB_{FH}$-DNA complexes are indicated at the right-hand side of the gel. The sizes of DNA marker fragments (M, lane 1; SmartLadder [Eurogentec]) are shown on the left-hand side of the gel in kb. (B) Binding of $RuvB_{Mge}$ to supercoiled plasmid DNA. Reactions were performed and analyzed using a method similar to that described for panel A and contained either 0 nM (−; lane 2), 340 nM (lane 3), 680 nM (lane 4), 1.35 μM (lane 5), 2.7 μM (lane 6), or 5.4 μM (lane 7) of $RuvB_{Mge}$. (C) Binding of $RuvB_{FH}$ to (6-FAM-labeled) HJ substrate HJ1.1 (33). Reactions were performed using a method similar to that described for panel A and contained either 0 nM (−; lanes 1 and 5), 1.35 μM (lanes 2 and 6), 2.7 μM (lanes 3 and 7), or 5.4 μM (lanes 4 and 8) of $RuvB_{FH}$. The reaction products were separated on a 5% polyacrylamide gel and analyzed by fluorometry. The reactions shown in lanes 5 to 8 (+Glut.) were treated with 0.25% glutaraldehyde (30 min at 37°C) after the binding reactions. The reactions shown in lanes 1 to 4 were not treated with glutaraldehyde (−Glut.) (D) Binding of $RuvB_{FH}$ to ssDNA (5′ 6-FAM-labeled oligonucleotide 1) (Fig. 3A). Reactions were performed using a method similar to that described in panel C. (E) Binding of $RuvB_{FH}$ to dsDNA (substrate VI; 5′ 6-FAM labeled on oligonucleotide 2/1) (Fig. 3A). Reactions were performed using a method similar to that described in panel C.

either ssDNA (Fig. 2D) or dsDNA (Fig. 2E). Similar results were obtained with the $RuvB_{Mge}$ protein (data not shown).

With respect to the binding to oligonucleotide substrates, the activities of $RuvB_{FH}$ and $RuvB_{Mge}$ differ in several important aspects from those of $RuvB_{Eco}$. First, in contrast to $RuvB_{FH}$ and $RuvB_{Mge}$, $RuvB_{Eco}$ requires $RuvA_{Eco}$ as well as Mg^{2+} for binding to HJs; this binding could be detected only after cross-linking with glutaraldehyde and resulted in large protein-DNA complexes that did not enter the polyacrylamide gels (25). Second, $RuvB_{Eco}$ did not appear to bind to other oligonucleotide substrates, such as duplex oligonucleotides, irrespective of the presence of $RuvA_{Eco}$ and divalent cations in the binding reactions (25).

$RuvB_{FH}$ and $RuvB_{Mge}$ have DNA helicase activity. To test the putative DNA helicase activity of $RuvB_{FH}$ and $RuvB_{Mge}$, both proteins were incubated with different types of DNA substrates. Schematic representations of the substrates, which have been described previously by Tsaneva et al. (40), are depicted in Fig. 3A. $RuvB_{FH}$ was found to readily unwind a DNA substrate consisting of a large single-stranded portion (φX174 virion DNA) to which a double-stranded oligonucleotide was annealed (Fig. 3A, substrate I). This activity was $RuvB_{FH}$ concentration, ATP, and Mg^{2+} dependent (see below) and resulted in the production of single-stranded oligonucleotides as well as (partially) double-stranded oligonucleotides (consisting of oligonucleotides 1 and 2) (Fig. 3B). The release of oligonucleotide 1 from the substrate was more efficient than that of oligonucleotide 2 (Fig. 3B, compare lanes 2 to 5, where oligonucleotide 1 of the substrate is labeled, to lanes 7 to 10, where oligonucleotide 2 is labeled). This result indicated that the DNA unwinding activity of $RuvB_{FH}$ has a preference regarding the polarity of the DNA substrate (see also below). Because $RuvB_{FH}$ was unable to unwind the (partial) duplexes consisting of oligonucleotides 1 and 2 in separate experiments (data not shown), we conclude that these duplexes represent end products from the unwinding of substrate 1 and cannot be processed further into the separate single-stranded oligonucleotides.

Apart from the discrete DNA products representing oligonucleotide 2 and the duplex of oligonucleotides 1 and 2, other, faint DNA products were generated with substrate I when oligonucleotide 2 was labeled (Fig. 3B, lanes 7 to 10, asterisk). The exact nature of these products, which migrated in the gel at a position intermediate to that of the single- and double-

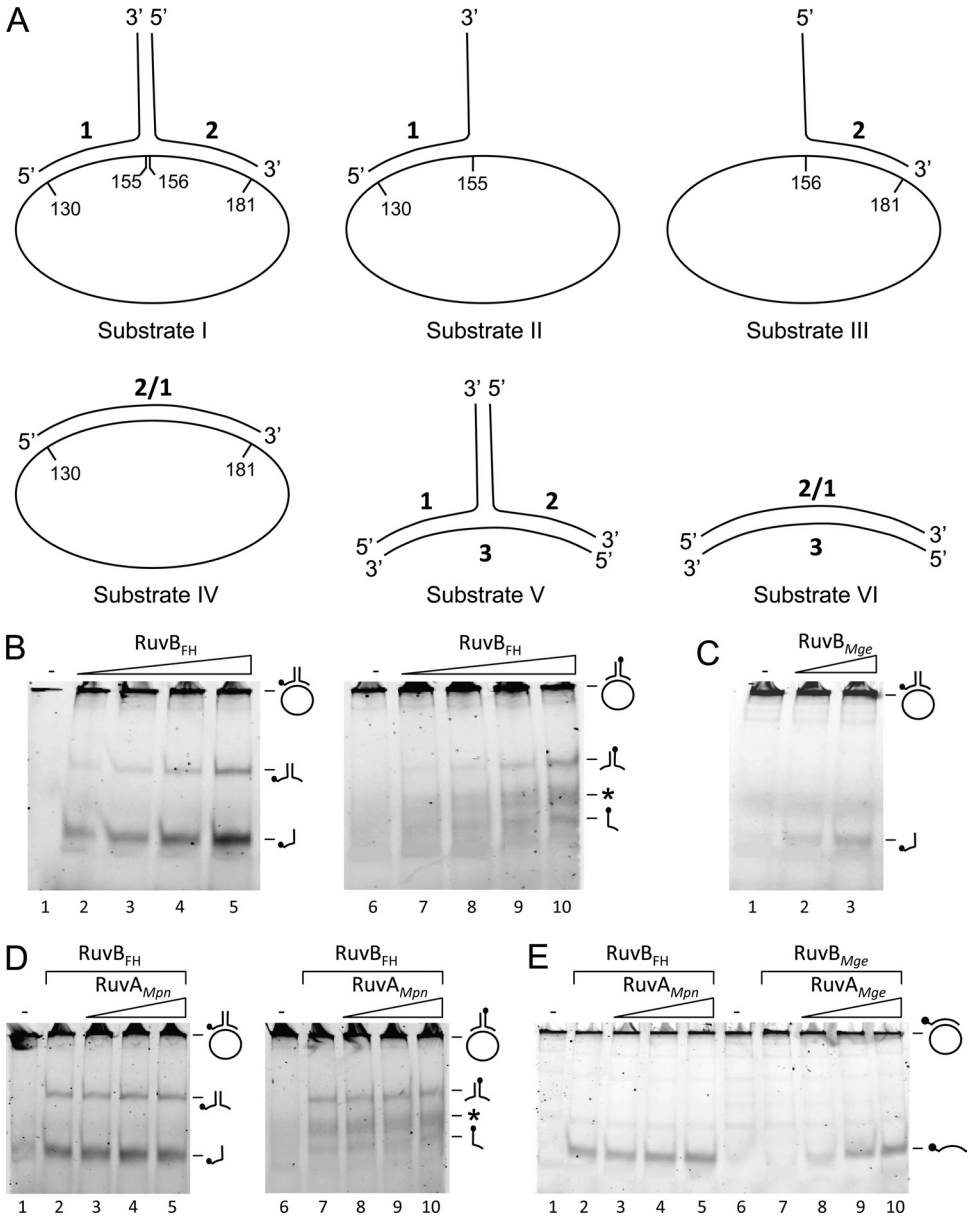

FIG. 3. DNA helicase activity of $RuvB_{FH}$ and $RuvB_{Mge}$. (A) Schematic illustration of the DNA substrates that were used in the DNA helicase assays. The substrates are composed of oligonucleotides (substrates V and VI) or a combination of oligonucleotides and single-stranded, circular 5,386-bp φX174 DNA (substrates I to IV). The φX174 DNA is pictured as an ellipse and is not drawn to scale with respect to the oligonucleotides. The sequences of the oligonucleotides (oligonucleotides 1, 2, 2/1, and 3) were described by Tsaneva et al. (40). (B) The activity of $RuvB_{FH}$ on substrate I. Substrate I, 6-FAM labeled at the 5′ end of either oligonucleotide 1 (lanes 1 to 5) or oligonucleotide 2 (lanes 6 to 10), was incubated with either 0 μM (−; lanes 1 and 6), 0.1 μM (lanes 2 and 7), 0.3 μM (lanes 3 and 8), 0.9 μM (lanes 4 and 9), or 2.7 μM (lanes 5 and 10) $RuvB_{FH}$ in the presence of Mg^{2+} (10 mM) and ATP (2 mM). After the reaction (5 min at 37°C), the samples were deproteinized, electrophoresed through native 12% polyacrylamide gels, and analyzed by fluorometry. The position of the substrate, which is too large to enter the gel, as well as the positions of the oligonucleotide reaction products, is indicated at the right-hand side of the gels by schematic illustrations. In these illustrations, the position of the 6-FAM label is indicated by a black circle. The asterisk points to DNA products in the gels that represent incorrectly annealed duplexes of unlabeled oligonucleotide 1, which is preferentially produced in the helicase reactions with substrate I, and labeled oligonucleotide 2 (see text). (C) The activity of $RuvB_{Mge}$ on substrate I. Substrate I, 6-FAM labeled at the 5′ end of oligonucleotide 1, was incubated with either 0 μM (−; lane 1), 0.9 μM (lane 2), or 2.7 μM (lane 3) of $RuvB_{Mge}$. The other reaction parameters were similar to those described for panel A. (D) $RuvA_{Mpn}$ does not influence the DNA helicase activity of $RuvB_{FH}$. Substrate I, 6-FAM labeled at the 5′ end of either oligonucleotide 1 (lanes 1 to 5) or oligonucleotide 2 (lanes 6 to 10), was incubated without protein (lanes 1 and 6) or with 2.7 μM $RuvB_{FH}$ in the presence of either 0 nM (lanes 2 and 7), 19 nM (lanes 3 and 8), 56 nM (lanes 4 and 9), or 167 nM (lanes 5 and 10) $RuvA_{Mpn}$. The other reaction parameters were similar to those described for panel A. The asterisk points to DNA products in the gels that represent incorrectly annealed duplexes of unlabeled oligonucleotide 1 and labeled oligonucleotide 2. (E) $RuvA_{Mpn}$-independent helicase activity of $RuvB_{FH}$ and $RuvA_{Mge}$-dependent helicase activity of $RuvB_{Mge}$. The activities of $RuvB_{FH}$ (lanes 2 to 5) and $RuvB_{Mge}$ (lanes 7 to 10) were tested on substrate IV in the presence of various concentrations of either $RuvA_{Mpn}$ or $RuvA_{Mge}$ (as indicated above the lanes) as follows: lanes 2 and 7, 0 nM; lanes 3 and 8, 56 nM; lanes 4 and 9, 167 nM; and lanes 5 and 10, 0.5 μM. The samples loaded in lanes 1 and 6 were incubated in the absence of any protein (−). The other reaction parameters were similar to those described in panel A.

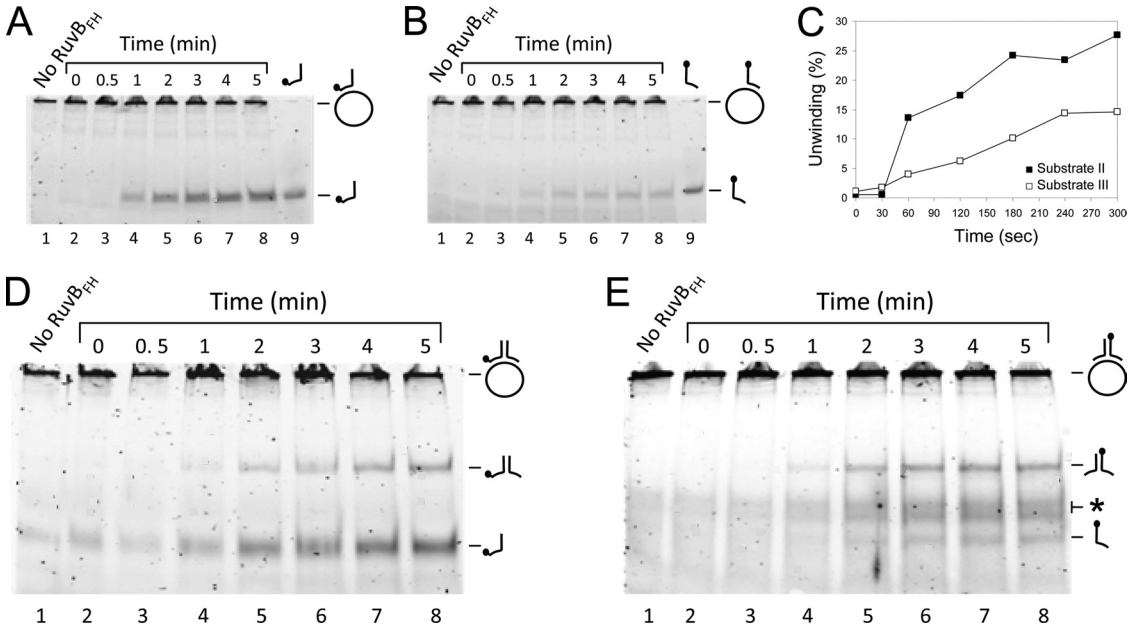

FIG. 4. Time course of the RuvB$_{FH}$-catalyzed DNA helicase reaction on different DNA substrates. The substrates that were tested were substrate II (A), substrate III (B), and substrate I, which was 6-FAM labeled at the 5′ end of either oligonucleotide 1 (D) or oligonucleotide 2 (E). Reactions were performed as described in the legend of Fig. 3 and contained either 0 μM RuvB$_{FH}$ or 2.7 μM RuvB$_{FH}$ in the presence of Mg^{2+} (10 mM) and ATP (2 mM). Samples were taken at the time points indicated above the lanes of the figures. The labeled oligonucleotides 1 and 2 are taken along as makers in panel A (lane 9) and panel B (lane 9), respectively. (C) Comparison of the percentage of unwinding (the percentage of displaced oligonucleotide) of substrate II (■) with that of substrate III (□). The displaced oligonucleotides were measured from the gels shown in panels A and B as the percentage of released product relative to the total substrate in the reaction mixture. The labeling of substrate and reaction products is similar to that used in Fig. 3.

stranded oligonucleotide products, is not known. However, as their formation depended on the presence of unlabeled oligonucleotide 1 in the substrate, it is likely that these products represent incorrectly annealed duplexes of unlabeled oligonucleotide 1, which is preferentially produced in the helicase reaction, and labeled oligonucleotide 2. This notion was corroborated by the observation that similar products were formed after labeled oligonucleotide 2 was mixed with unlabeled oligonucleotide 1 at relatively low temperatures (≤37°C) (data not shown).

Like the RuvB$_{FH}$ protein, RuvB$_{Mge}$ also displayed DNA unwinding activity. This activity, however, was significantly lower than that of its *M. pneumoniae* ortholog (Fig. 3C, lanes 2 and 3). This finding corresponded with the results from the ATPase assay, in which RuvB$_{Mge}$ was found to have a lower activity than RuvB$_{FH}$ (Fig. 1C).

The DNA helicase activities of both RuvB$_{FH}$ and RuvB$_{Mge}$ are remarkable as the counterpart of these proteins from *E. coli*, RuvB$_{Eco}$, was previously reported to be incapable of DNA unwinding by itself (39). Although the RuvB$_{Eco}$ protein does have intrinsic DNA helicase activity, the protein is able to exert this activity only in the presence of RuvA$_{Eco}$ (39). To investigate whether the RuvA homologues from *M. pneumoniae* and *M. genitalium* (RuvA$_{Mpn}$ and RuvA$_{Mge}$, respectively) can influence the activities of RuvB$_{FH}$ and RuvB$_{Mge}$, various concentrations of the RuvA proteins were included in helicase assays using a range of DNA substrates. As shown in Fig. 3D, the helicase activity of RuvB$_{FH}$ on substrate I was not changed significantly by RuvA$_{Mpn}$. We were also unable to detect a significant effect of RuvA$_{Mpn}$ on RuvB$_{FH}$ activity with other DNA substrates and at different RuvB$_{FH}$ concentrations (Fig. 3E, lanes 2 to 5, and data not shown). In contrast, the RuvB$_{Mge}$ protein did show an RuvA$_{Mge}$-dependent effect although this effect was observed only with one of the substrates that was employed in this study, i.e., substrate IV. While RuvB$_{Mge}$ alone was unable to unwind this substrate (Fig. 3E, lane 7), the protein displaced the substrate in the presence of RuvA$_{Mge}$. This stimulatory effect of RuvA$_{Mge}$ on RuvB$_{Mge}$ was RuvA$_{Mge}$ concentration dependent (Fig. 3E, lanes 7 to 10). Like RuvA$_{Mpn}$ and RuvA$_{Eco}$ (39), RuvA$_{Mge}$ alone was unable to catalyze DNA strand displacement (data not shown). Thus, while the DNA helicase activity of RuvB$_{FH}$ is not dependent on RuvA$_{Mpn}$, the helicase activity of RuvB$_{Mge}$ is RuvA$_{Mge}$ dependent on specific DNA substrates. In this respect, the activity of RuvB$_{Mge}$ plus RuvA$_{Mge}$ resembles that of the RuvAB helicase from *E. coli* (RuvAB$_{Eco}$) (39).

Both RuvB$_{FH}$ and RuvB$_{Mge}$ were unable to unwind HJ substrates and double-stranded oligonucleotide substrates, such as substrates V and VI (Fig. 3A), irrespective of the presence of RuvA$_{Mpn}$ or RuvA$_{Mge}$ in the reaction mixture (data not shown).

Time course of the RuvB$_{FH}$-catalyzed helicase reaction. As the RuvB$_{FH}$ protein appears to have unique characteristics in comparison to RuvB$_{Mge}$ and RuvB$_{Eco}$, we investigated the time course as well as the reaction requirements of the helicase activity of this protein on substrates I, II, and III. Substrate II, consisting of oligonucleotide 1 annealed to φX174 single-stranded DNA, was most efficiently unwound by RuvB$_{FH}$ (Fig. 4A). Under the

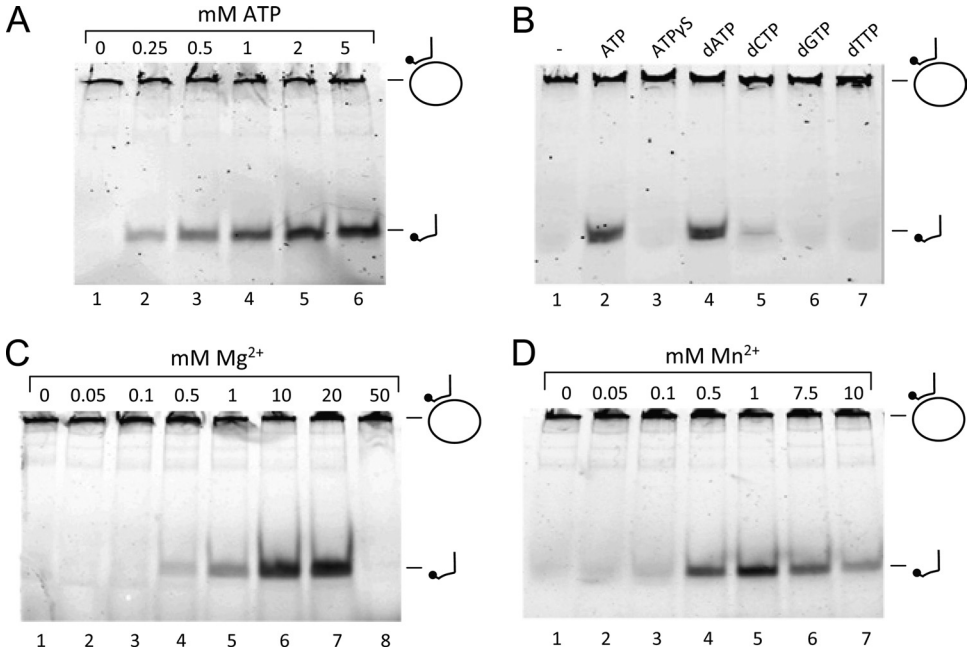

FIG. 5. Reaction requirements of the $RuvB_{FH}$-catalyzed DNA helicase reaction. (A) ATP dependence of the DNA helicase activity of $RuvB_{FH}$. Reactions with substrate II and 2.7 μM $RuvB_{FH}$ were performed in the absence (lane 1) or presence of ATP at a concentration of either 0.25, 0.5, 1, 2, or 5 mM (as indicated above the lanes). (B) Nucleotide cofactor dependence of the DNA helicase activity of $RuvB_{FH}$. Reactions with substrate II and 2.7 μM $RuvB_{FH}$ were performed in the absence (lane 1) or presence of a 2 mM concentration of either ATP (lane 2), ATPγS (lane 3), dATP (lane 4), dCTP (lane 5), dGTP (lane 6), or dTTP (lane 7). (C) Mg^{2+} dependence of the DNA helicase activity of $RuvB_{FH}$. Reactions with substrate II and 2.7 μM $RuvB_{FH}$ were performed in the absence (lane 1) or presence of various concentrations of Mg^{2+} (as indicated above the lanes). (D) Reactions with substrate II and 2.7 μM $RuvB_{FH}$ were performed in the absence (lane 1) or presence of various concentrations of Mn^{2+} (as indicated above the lanes). The labeling of substrate and reaction products is similar to that used in Fig. 3.

specific test conditions, maximal levels of 25 to 30% were reached after 3 min of incubation (Fig. 4A and C). Substrate III was less efficiently unwound by $RuvB_{FH}$ than substrate II: approximately 15% of this substrate was displaced after 4 min of incubation (Fig. 4B and C). These results corresponded with the results obtained with substrate I, from which oligonucleotide 1 was more efficiently displaced than oligonucleotide 2 (compare Fig. 4D and E). As expected, the efficiency by which the partial duplex of oligonucleotides 1 and 2 was displaced from substrate I was not influenced by the position of the fluorescent label: a similar time course of production of the duplex was seen when either oligonucleotide 1 (Fig. 4D) or oligonucleotide 2 (Fig. 4E) was labeled. The preferential displacement of oligonucleotide 1 from substrate I by $RuvB_{FH}$ is similar to that reported for $RuvAB_{Eco}$. The preferred polarity of the helicase activity of the latter enzyme complex was found to be $5' \rightarrow 3'$ with respect to the (long) single-stranded part of a branched or partially double-stranded substrate (39, 40).

Reaction requirements of the $RuvB_{FH}$-catalyzed DNA helicase reaction. We previously found $RuvB_{FH}$ and $RuvB_{Mge}$ to have ATPase activity (Fig. 1C). To investigate the ATP dependence of the helicase activity of $RuvB_{FH}$, the protein's activity on substrate II was tested in the presence of various concentrations of ATP. As shown in Fig. 5A, the protein is inactive in the absence of ATP in the reaction mixture (lane 1). However, in the presence of ATP (0.25 mM or higher), $RuvB_{FH}$ readily unwound the substrate, with optimal activities reached at a concentration of ~2 mM ATP. The dependence of $RuvB_{FH}$ activity on the hydrolysis of ATP is further demonstrated by the inactivity of the protein in the presence of the nonhydrolyzable analog of ATP, ATPγS [adenosine 5′-*O*-(3-thio)triphosphate] (Fig. 5B, lane 3). In the presence of dATP, however, the protein exhibited similar activities as in the presence of ATP (lane 4). Nucleotide cofactor dCTP was also able to support $RuvB_{FH}$ activity, albeit at a relatively low level (lane 5). The protein did not display significant activity in the presence of either dGTP or dTTP (Fig. 5B, lanes 6 and 7). This pattern of nucleotide cofactor dependence is highly similar to that reported for the HJ dissociation activity of $RuvAB_{Eco}$ (24).

Like numerous other enzymes that interact with DNA, $RuvB_{FH}$ and $RuvB_{Mge}$ require divalent cations for activity. $RuvB_{FH}$ was found to be active at ≥0.5 mM concentrations of either Mg^{2+} (Fig. 5C, lane 4) or Mn^{2+} (Fig. 5D, lane 4). The optimal concentrations of these divalent cations for stimulation of $RuvB_{FH}$ were ~10 mM for Mg^{2+} (Fig. 5C, lane 6) and ~1 mM for Mn^{2+} (Fig. 5D, lane 5).

Comparison of the DNA helicase activities of $RuvB_{FH}$ and $RuvB_{M129}$. As described above, the $RuvB_{FH}$ protein can be expressed only by *M. pneumoniae* strains that belong to the subtype 2 genotype. Conversely, subtype 1 strains were found to express a RuvB version ($RuvB_{M129}$) with a single amino acid residue substitution in comparison with $RuvB_{FH}$ (at position 140) (Fig. 1A). Because the Trp residue at position 140 of $RuvB_{M129}$ is not conserved among bacterial RuvB sequences and, more importantly, because this residue is contained within the highly conserved sensor I motif of AAA^+ proteins, we

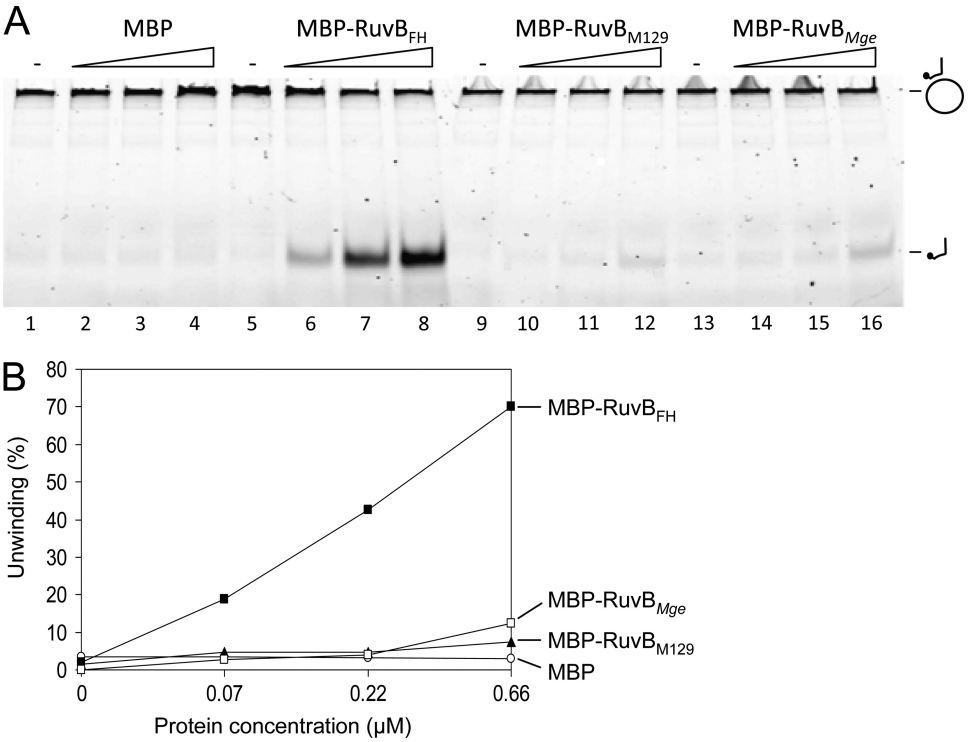

FIG. 6. DNA helicase activities of MBP fusion proteins of RuvB$_{FH}$, RuvB$_{M129}$, and RuvB$_{Mge}$. (A) DNA helicase activities of MBP-RuvB$_{FH}$, MBP-RuvB$_{M129}$, and MBP-RuvB$_{Mge}$. Reactions were performed with substrate II and various concentrations of MBP-β-galactosidase-α (MBP; lanes 2 to 4), MBP-RuvB$_{FH}$ (lanes 6 to 8), MBP-RuvB$_{M129}$ (lanes 10 to 12), and MBP-RuvB$_{Mge}$ (lanes 14 to 16). Each protein was tested at a concentration of 0.07, 0.22, and 0.66 μM (as indicated by the triangles above the lanes). (B) The percentage of unwinding (the percentage of displaced oligonucleotide) of substrate II by MBP-RuvB$_{FH}$ (■), MBP-RuvB$_{Mge}$ (□), MBP-RuvB$_{M129}$ (▲), and MBP (○). The displaced oligonucleotides were measured from the gel shown in panel A as the percentage of released product relative to the total substrate in the reaction mixture.

anticipated that RuvB$_{M129}$ could have significantly different features than RuvB$_{FH}$. To investigate this notion, we set out to purify RuvB$_{M129}$ in its native state after overexpression of the protein in *E. coli*, in a similar fashion as described above for RuvB$_{FH}$ and RuvB$_{Mge}$. Nevertheless, while RuvB$_{M129}$ could be expressed to high levels, the protein turned out to be extremely insoluble. After using different protocols of solubilization, including denaturation and renaturation procedures, we were unable to obtain sufficient amounts of soluble RuvB$_{M129}$ to allow its purification. Because the expression of proteins as fusions to maltose-binding protein (MBP) can often resolve problems related to improper protein folding or insolubility (31, 33, 42–43), we expressed and purified RuvB$_{M129}$, as well as RuvB$_{FH}$ and RuvB$_{Mge}$, as MBP fusion proteins. As shown in Fig. 6A (lanes 6 to 8), the fusion of MBP and RuvB$_{FH}$ (MBP-RuvB$_{FH}$) displayed protein concentration-dependent DNA helicase activity similar to that of RuvB$_{FH}$. Similarly, the activity of MBP-RuvB$_{Mge}$ corresponded with that of its native counterpart, being significantly lower than that of MBP-RuvB$_{FH}$ (Fig. 6A, lanes 14 to 16, and B). Interestingly, MBP-RuvB$_{M129}$ also displayed DNA helicase activity although this activity was only slightly higher than that observed for MBP, which served as a negative control (Fig. 6A, compare lanes 10 to 12 to lanes 2 to 4, and B). We conclude that RuvB$_{M129}$ possesses DNA helicase activity even though this activity is significantly lower than that of RuvB$_{FH}$.

DISCUSSION

We have characterized the RuvB homologs from *M. pneumoniae* and *M. genitalium* and found these proteins to have several exceptional features compared to the well-characterized RuvB protein from *E. coli*. The most remarkable activity was exhibited by the RuvB$_{FH}$ protein. This protein was found to function as a potent divalent cation- and ATP-dependent DNA helicase in the absence of any protein cofactor, such as RuvA. In contrast, RuvB$_{Eco}$ was previously found to mediate DNA unwinding exclusively in the presence of RuvA$_{Eco}$ (39, 40). In this respect, the DNA helicase activity of RuvB$_{Eco}$ differs from its HJ branch migration activity as the latter activity was also found to proceed in the absence of RuvA at high concentrations of both RuvB$_{Eco}$ and Mg^{2+} (20, 38).

The DNA helicase activity of RuvB$_{FH}$ appeared to have a polarity similar to that of RuvAB$_{Eco}$, which was reported to preferentially unwind DNA in the direction 5′ → 3′ with respect to the (relatively long) single-stranded portion of a partially double-stranded DNA substrate (39, 40). Interestingly, in contrast to RuvAB$_{Eco}$ (40), RuvB$_{FH}$ was unable to displace three-armed double-stranded oligonucleotide substrates, such as substrate V (Fig. 3A), in either the absence or the presence of RuvA$_{Mpn}$ (data not shown). This indicated that RuvB$_{FH}$ is capable of unwinding only DNA substrates that are partially double stranded. Moreover, four-armed double-stranded

DNA substrates that resembled HJs were also not processed by $RuvB_{FH}$, irrespective of the presence of $RuvA_{Mpn}$ in the reaction mixture (data not shown). Such substrates, however, were reported to be readily dissociated by $RuvAB_{Eco}$ through branch migration (14, 24, 25). The inability of $RuvB_{FH}$ to unwind HJ substrates may be caused by the apparent inability of the protein to interact directly with $RuvA_{Mpn}$. This view is based on the crucial role that is played by $RuvA_{Eco}$ (as part of the $RuvAB_{Eco}$ complex) in the recognition and processing of HJs (14, 24, 30, 46).

Regarding the interaction between RuvB and RuvA proteins, it is important that the region of $RuvB_{Eco}$ that was found to be crucial for binding to $RuvA_{Eco}$ is localized between amino acid residues 134 and 153; this region consists of a β-hairpin (Fig. 1A, β-hairpin 1) that protrudes from the AAA^+ ATPase domain of the protein (7, 45). As described in Results, the sequence of the β-hairpin 1 is not highly conserved between $RuvB_{Eco}$ and the RuvB sequences from *Mycoplasma* spp. Also, two of the amino acid residues within the β-hairpin 1 of $RuvB_{Eco}$ that were reported to be crucial for the functional and physical interaction of the protein with $RuvA_{Eco}$ (Ile148 and Ile150) (7) are not conserved in $RuvB_{FH}$, $RuvB_{M129}$, or $RuvB_{Mge}$. While protein-protein interactions are not exclusively defined by primary protein structure, it is tempting to speculate that the incapacity of $RuvB_{FH}$ and $RuvB_{M129}$ to be stimulated by $RuvA_{Mpn}$ is determined by the inability of these proteins to physically interact. Obviously, this hypothetical failure to interact may be caused by sequences in both RuvB and RuvA. In this regard, it is interesting that $RuvA_{Mpn}$ could not complement a *ruvA*-deficient *E. coli* mutant and did not stimulate the branch migration activity of $RuvB_{Eco}$ *in vitro* (9). Nevertheless, in contrast to its *M. pneumoniae* orthologs, the *M. genitalium* RuvB protein did show $RuvA_{Mge}$-dependent DNA helicase activity on a specific DNA substrate (Fig. 3E). This result indicated that $RuvB_{Mge}$ can functionally interact with $RuvA_{Mge}$. It is yet unclear, however, why this stimulatory effect of $RuvA_{Mge}$ was observed with only a single substrate.

Another fascinating finding that came out of this study was the difference in characteristics between the RuvB protein expressed by subtype 2 *M. pneumoniae* strains ($RuvB_{FH}$) and that expressed by subtype 1 strains ($RuvB_{M129}$). While $RuvB_{FH}$ was expressed in *E. coli* as a soluble protein that could readily be purified, the $RuvB_{M129}$ protein was found to be highly insoluble. As a consequence, we were unable to purify this protein. It could be purified, however, as an MBP fusion protein, in a similar fashion as $RuvB_{FH}$ and $RuvB_{Mge}$. Thus, we were able to demonstrate that the MBP-$RuvB_{M129}$ protein does have DNA helicase activity, albeit dramatically less than that of MBP-$RuvB_{FH}$ (or $RuvB_{FH}$). It is remarkable that the dissimilarity between $RuvB_{FH}$ and $RuvB_{M129}$ is caused by a single residue difference in their amino acid sequences: $RuvB_{FH}$ has a Leu residue at position 140, whereas $RuvB_{M129}$ carries a Trp residue at that position. Residue Leu140, which corresponds to Leu157 in $RuvB_{Eco}$, is highly conserved among virtually all known RuvB sequences and forms part of the (putative) sensor I sequence (Fig. 1A). The importance of this protein motif was previously demonstrated for $RuvB_{Eco}$ by mutagenesis of the invariant sensor I residues Gly159, Ala160, T161, and T162 (12). Mutations in each of these residues resulted in proteins with significantly reduced *in vivo* DNA repair activities (12). We here show that another conserved residue from the putative sensor I sequence, Leu140 in $RuvB_{FH}$, is also important for RuvB function, at least *in vitro*. By combining the *in vivo* properties of the $RuvB_{Eco}$ sensor I mutants (12) with the characteristics of $RuvB_{FH}$ and $RuvB_{M129}$ reported here, we would expect RuvB function to be considerably impaired in *M. pneumoniae* subtype 1 strains as opposed to subtype 2 strains. This could have a significant impact on the functionality or efficiency of the DNA recombination and repair machinery in subtype 1 strains. Whether subtype 1 and subtype 2 strains, indeed, differ in this respect is yet unknown. Moreover, we cannot rule out the possibility that native $RuvB_{M129}$ is expressed in a soluble and active form in *M. pneumoniae* subtype 1 strains. Clearly, these notions should be investigated further by the generation of MPN536 knockouts and reciprocal knock-ins in strains that are derived from both genetic lineages of *M. pneumoniae*. Such experiments are currently being designed, despite the limited availability of tools for the genetic manipulation of *M. pneumoniae*.

In conclusion, this study once again underlines the major differences that exist between the components of the DNA recombination and repair machinery of *Mycoplasma* spp. and those of Gram-positive and Gram-negative bacteria. As a consequence, great care should be taken in the attribution of function to specific gene products on the sole basis of sequence similarities.

ACKNOWLEDGMENTS

We thank E. Spuesens for critically reading the manuscript.

A.M.C.V.R. is supported by grants of the European Society for Pediatric Infectious Diseases, ZonMW, and the Erasmus MC.

REFERENCES

1. Reference deleted.
2. **Carvalho, F. M., et al.** 2005. DNA repair in reduced genome: the *Mycoplasma* model. Gene **360:**111–119.
3. **Dandekar, T., et al.** 2000. Re-annotating the *Mycoplasma pneumoniae* genome sequence: adding value, function and reading frames. Nucleic Acids Res. **28:**3278–3288.
4. **Davey, M. J., D. Jeruzalmi, J. Kuriyan, and M. O'Donnell.** 2002. Motors and switches: AAA^+ machines within the replisome. Nat. Rev. Mol. Cell Biol. **3:**826–835.
5. Reference deleted.
6. **Fraser, C. M., et al.** 1995. The minimal gene complement of *Mycoplasma genitalium*. Science **270:**397–403.
7. **Han, Y. W., et al.** 2001. A unique beta-hairpin protruding from AAA^+ ATPase domain of RuvB motor protein is involved in the interaction with RuvA DNA recognition protein for branch migration of Holliday junctions. J. Biol. Chem. **276:**35024–35028.
8. **Himmelreich, R., et al.** 1996. Complete sequence analysis of the genome of the bacterium *Mycoplasma pneumoniae*. Nucleic Acids Res. **24:**4420–4449.
9. **Ingleston, S. M., et al.** 2002. Holliday junction binding and processing by the RuvA protein of *Mycoplasma pneumoniae*. Eur. J. Biochem. **269:**1525–1533.
10. **Iverson-Cabral, S. L., S. G. Astete, C. R. Cohen, E. P. Rocha, and P. A. Totten.** 2006. Intrastrain heterogeneity of the *mgpB* gene in *Mycoplasma genitalium* is extensive in vitro and in vivo and suggests that variation is generated via recombination with repetitive chromosomal sequences. Infect. Immun. **74:**3715–3726.
11. **Iverson-Cabral, S. L., S. G. Astete, C. R. Cohen, and P. A. Totten.** 2007. *mgpB* and *mgpC* sequence diversity in *Mycoplasma genitalium* is generated by segmental reciprocal recombination with repetitive chromosomal sequences. Mol. Microbiol. **66:**55–73.
12. **Iwasaki, H., et al.** 2000. Mutational analysis of the functional motifs of RuvB, an AAA^+ class helicase and motor protein for Holliday junction branch migration. Mol. Microbiol. **36:**528–538.
13. **Iwasaki, H., T. Shiba, K. Makino, A. Nakata, and H. Shinagawa.** 1989. Overproduction, purification, and ATPase activity of the *Escherichia coli* RuvB protein involved in DNA repair. J. Bacteriol. **171:**5276–5280.
14. **Iwasaki, H., M. Takahagi, A. Nakata, and H. Shinagawa.** 1992. *Escherichia coli* RuvA and RuvB proteins specifically interact with Holliday junctions and promote branch migration. Genes Dev. **6:**2214–2220.

15. **Kenri, T., et al.** 1999. Identification of a new variable sequence in the P1 cytadhesin gene of *Mycoplasma pneumoniae*: evidence for the generation of antigenic variation by DNA recombination between repetitive sequences. Infect. Immun. **67:**4557–4562.
16. **Laemmli, U. K.** 1970. Cleavage of structural proteins during the assembly of the head of bacteriophage T4. Nature **227:**680–685.
17. **Ma, L., et al.** 2007. *Mycoplasma genitalium*: an efficient strategy to generate genetic variation from a minimal genome. Mol. Microbiol. **66:**220–236.
18. **Maquelin, K., et al.** 2009. Raman spectroscopic typing reveals the presence of carotenoids in *Mycoplasma pneumoniae*. Microbiology **155:**2068–2077.
19. **Morimatsu, K., M. Takahashi, and B. Norden.** 2002. Arrangement of RecA protein in its active filament determined by polarized-light spectroscopy. Proc. Natl. Acad. Sci. U. S. A. **99:**11688–11693.
20. **Muller, B., I. R. Tsaneva, and S. C. West.** 1993. Branch migration of Holliday junctions promoted by the *Escherichia coli* RuvA and RuvB proteins. I. Comparison of RuvAB- and RuvB-mediated reactions. J. Biol. Chem. **268:** 17179–17184.
21. **Muller, B., I. R. Tsaneva, and S. C. West.** 1993. Branch migration of Holliday junctions promoted by the *Escherichia coli* RuvA and RuvB proteins. II. Interaction of RuvB with DNA. J. Biol. Chem. **268:**17185–17189.
22. **Neuwald, A. F., L. Aravind, J. L. Spouge, and E. V. Koonin.** 1999. AAA^+: a class of chaperone-like ATPases associated with the assembly, operation, and disassembly of protein complexes. Genome Res. **9:**27–43.
23. **Ohnishi, T., T. Hishida, Y. Harada, H. Iwasaki, and H. Shinagawa.** 2005. Structure-function analysis of the three domains of RuvB DNA motor protein. J. Biol. Chem. **280:**30504–30510.
24. **Parsons, C. A., I. Tsaneva, R. G. Lloyd, and S. C. West.** 1992. Interaction of *Escherichia coli* RuvA and RuvB proteins with synthetic Holliday junctions. Proc. Natl. Acad. Sci. U. S. A. **89:**5452–5456.
25. **Parsons, C. A., and S. C. West.** 1993. Formation of a RuvAB-Holliday junction complex in vitro. J. Mol. Biol. **232:**397–405.
26. **Peterson, S. N., et al.** 1995. Characterization of repetitive DNA in the *Mycoplasma genitalium* genome: possible role in the generation of antigenic variation. Proc. Natl. Acad. Sci. U. S. A. **92:**11829–11833.
27. **Peterson, S. N., P. C. Hu, K. F. Bott, and C. A. Hutchison, 3rd.** 1993. A survey of the *Mycoplasma genitalium* genome by using random sequencing. J. Bacteriol. **175:**7918–7930.
28. **Putnam, C. D., et al.** 2001. Structure and mechanism of the RuvB Holliday junction branch migration motor. J. Mol. Biol. **311:**297–310.
29. **Ruland, K., R. Wenzel, and R. Herrmann.** 1990. Analysis of three different repeated DNA elements present in the P1 operon of *Mycoplasma pneumoniae*: size, number and distribution on the genome. Nucleic Acids Res. **18:**6311–6317.
30. **Shiba, T., H. Iwasaki, A. Nakata, and H. Shinagawa.** 1991. SOS-inducible DNA repair proteins, RuvA and RuvB, of *Escherichia coli*: functional interactions between RuvA and RuvB for ATP hydrolysis and renaturation of the cruciform structure in supercoiled DNA. Proc. Natl. Acad. Sci. U. S. A. **88:**8445–8449.
31. **Sluijter, M., M. Aslam, N. G. Hartwig, A. M. van Rossum, and C. Vink.** 2011. Identification of amino acid residues critical for catalysis of Holliday junction resolution by *Mycoplasma genitalium* RecU. J. Bacteriol. **193:**3941–3948.
32. **Sluijter, M., T. Hoogenboezem, N. G. Hartwig, and C. Vink.** 2008. The *Mycoplasma pneumoniae* MPN229 gene encodes a protein that selectively binds single-stranded DNA and stimulates recombinase A-mediated DNA strand exchange. BMC Microbiol. **8:**167.
33. **Sluijter, M., et al.** 2010. The *Mycoplasma genitalium* MG352-encoded protein is a Holliday junction resolvase that has a non-functional orthologue in *Mycoplasma pneumoniae*. Mol. Microbiol. **77:**1261–1277.
34. **Sluijter, M., E. B. Spuesens, N. G. Hartwig, A. M. van Rossum, and C. Vink.** 2009. The *Mycoplasma pneumoniae* MPN490 and *Mycoplasma genitalium* MG339 genes encode RecA homologs that promote homologous DNA strand exchange. Infect. Immun. **77:**4905–4911.
35. **Spuesens, E. B., N. G. Hartwig, A. M. van Rossum, and C. Vink.** 2010. Identification and classification of P1 variants of *Mycoplasma pneumoniae*. J. Clin. Microbiol. **48:**680.
36. **Spuesens, E. B., et al.** 2009. Sequence variations in RepMP2/3 and RepMP4 elements reveal intragenomic homologous DNA recombination events in *Mycoplasma pneumoniae*. Microbiology **155:**2182–2196.
37. **Su, C. J., A. Chavoya, and J. B. Baseman.** 1988. Regions of *Mycoplasma pneumoniae* cytadhesin P1 structural gene exist as multiple copies. Infect. Immun. **56:**3157–3161.
38. **Tsaneva, I. R., B. Muller, and S. C. West.** 1992. ATP-dependent branch migration of Holliday junctions promoted by the RuvA and RuvB proteins of *E. coli*. Cell **69:**1171–1180.
39. **Tsaneva, I. R., B. Muller, and S. C. West.** 1993. RuvA and RuvB proteins of *Escherichia coli* exhibit DNA helicase activity in vitro. Proc. Natl. Acad. Sci. U. S. A. **90:**1315–1319.
40. **Tsaneva, I. R., and S. C. West.** 1994. Targeted versus non-targeted DNA helicase activity of the RuvA and RuvB proteins of *Escherichia coli*. J. Biol. Chem. **269:**26552–26558.
41. Reference deleted.
42. **Vink, C., A. M. Oude Groeneger, and R. H. Plasterk.** 1993. Identification of the catalytic and DNA-binding region of the human immunodeficiency virus type I integrase protein. Nucleic Acids Res. **21:**1419–1425.
43. **Vink, C., K. H. van der Linden, and R. H. Plasterk.** 1994. Activities of the feline immunodeficiency virus integrase protein produced in Escherichia coli. J. Virol. **68:**1468–1474.
44. **Wenzel, R., and R. Herrmann.** 1988. Repetitive DNA sequences in *Mycoplasma pneumoniae*. Nucleic Acids Res. **16:**8337–8350.
45. **Yamada, K., et al.** 2001. Crystal structure of the Holliday junction migration motor protein RuvB from *Thermus thermophilus* HB8. Proc. Natl. Acad. Sci. U. S. A. **98:**1442–1447.
46. **Yamada, K., et al.** 2002. Crystal structure of the RuvA-RuvB complex: a structural basis for the Holliday junction migrating motor machinery. Mol. Cell **10:**671–681.